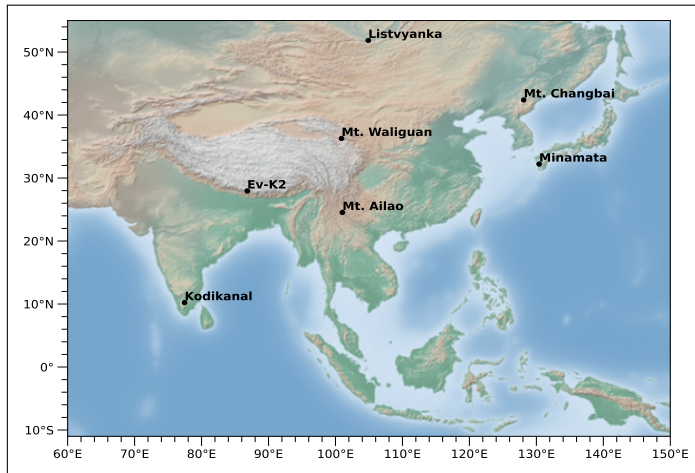


# Supplementary Information for "Modeling of Mercury Deposition in India: Evaluating Emission Inventories and Anthropogenic Impacts"

**CHAKRADHAR REDDY MALASANI**

Mercury (Hg), a ubiquitous atmospheric trace metal posing serious health risks, originates from natural and anthropogenic sources. India, the world's second-largest Hg emitter and a signatory to the Minamata Convention is committed to reducing emissions. However, spatio-temporal data on Hg distribution across the vast Indian subcontinent remains scarce. This study addresses this gap by employing the GEOS-Chem model with various emission inventories (UNEP2010, WHET, EDGAR, STREETS, UNEP2015) to simulate Hg variability across India from 2013 to 2017. Model performance was evaluated using ground-based GMOS observations and literature data. Emission inventory performance varied across stations. Hence, we employed ensemble-averaged results from all inventories. The maximum relative bias for TGM and GEM concentrations is about  $\pm 20\%$ , indicating simulations with sufficient accuracy. Hg wet deposition fluxes are highest over the Western Ghats and the Himalayan foothills due to higher rainfall. During the monsoon, the Hg wet deposition flux is about 65.4% of the annual wet deposition flux. Moreover, westerly winds cause higher wet deposition in summer over northern and eastern India. Hg Dry Deposition flux accounts for 72-74% of total deposition over India. Hg dry deposition fluxes are higher over eastern India, which correlates strongly with the leaf area index. Excluding Indian anthropogenic emissions from the model simulations resulted in a substantial decrease (21.9% and 33.5%) in wet and dry Hg deposition fluxes, highlighting the dominant role of human activities in Hg pollution in India.

## 1. METHODOLOGY



**Fig. S1.** Location of GMOS (Global Mercury Observation System) stations in the Asian domain considered for our study. Kodaikanal is the only station located in India. Data from these stations for 2013-2017 have been used to validate the GEOS-Chem model results.

## 2. VALIDATION

**Table S1.** Observed surface Hg concentrations from various research articles within the GC model nested asian domain

Site	Location		Altitude	Type	Monitoring period	Observation			References
	Lon	Lat				GEM (ng/m <sup>3</sup> )	RGM (pg/m <sup>3</sup> )	PBM (pg/m <sup>3</sup> )	
Mt. Aliao	101.03°	24.54°		Remote	2/2013-12/2013			2.24	[1]
Mt. Changbai (2013)	128.112°	42.402°	740	Remote	1/2013-12/2013	1.73	18.9	5.7	[2]
Mt. Changbai (2014)	128.112°	42.402°	740	Remote	1/2014-12/2014	1.58			[3]
Mt. Changbai (2015)	128.112°	42.402°	740	Remote	1/2015-12/2015	1.60			[3]
Mt. Qomolangma	86.93°	28.35°	4276	Remote	4-8/2016	1.42	25.6	21.4	[4]
Mt. Damei	121.565°	29.632°	550	Remote	4/2013-4/2014	3.31	154	6.3	[5]
Mt.waliguan	100.9°	36.29°	550	Remote	2/2013-6/2013				18.1 [? ]
Nam Co Lake	90.989°	30.774°	4730	Remote	11/2014-2/2015	0.95	48.96	0.85	[6]
Changdao	119.589°	39.949°	3	Remote	1/2014-7/2015	2.3			[7]
Changdao	119.589°	39.949°	3	Remote	1/2013-7/2015	2.52	28.0	9.3	[8]
Bayinbuluk	83.717°	42.893°	2430	Remote	1/2014-12/2014	1.62			[9]
Miyun2016	116.775°	40.481°	220	Rural	4/2016-10/2016	3.14	48.58	34.68	[9]
Lulin	120.87°	23.47°	2862	Remote	1/2013-12/2016	1.60	3.1	15.0	[10][11]
Chongming (2014)	121.908°	31.522°	11	Remote	3/2014-12/2014	2.7	23.0	15.2	[12]
Chongming (2015)	121.908°	31.522°	11	Remote	1/2015-12/2015	2.2	9.7	8.1	[12]
Chongming (2016)	121.908°	31.522°	11	Remote	1/2016-12/2016	1.8	21.8	19.2	[12]
Chongming (2017)	121.909°	31.523°	11	Remote	1/2017-12/2017	1.8	43.1	11.3	[12]
Qingdao1	120.5°	36.16°	40	Urban	1/2013	2.80	245		[13]
Shanghai1	121.436°	31.025°	300	Urban	12/2013-1/2014	3.42			[14]
Shanghai2	120.99°	31.10°	17	Urban	6-12/2013	4.19	197.8	21.1	[15]
Shanghai3	121.40°	31.22°	14	Urban	6/2015-5/2016	2.77	60.8	82.13	[16]
Jinan	117.03°	36.67°	7	Urban	10/2015-7/2016	4.91	452		[17]
Ningbo1	121.544°	29.86°	10	Urban	1/2013	3.79			[9]
Ningbo2	121.895°	29.75°	15	Urban	12/2016-11/2017	2.44			[18]
Ningbo3	121.81°	29.89°	15	Urban	2/2013-1/2014	3.26	659	197	[19]
Nanjing	118.95°	32.12°	30	Urban	8/2014-7/2015	3.85	127.4	43	[9]
Hefei	117.17°	31.52°	20	Urban	7/2013-6/2014	4.07	30	3.67	[20]
Chongqing	106.67°	29.62°	300	Urban	3-12/2014	3.51			[21]
Beijing (2015)	116.36°	39.98°	110	Urban	4/2015-12/2015	4.7			[22]
Beijing (2016)	116.36°	39.98°	110	Urban	1/2016-12/2016	3.5			[22]
Beijing (2017)	116.36°	39.98°	110	Urban	1/2017-12/2017	3.1			[22]
Beijing1	116.33°	40°	56	Urban	12/2016-11/2017	4.5	74.2	46.3	[9]
Chennai	80.237°	13.07°		Urban	02/2016-12/2016	4.66			[23]

**Table S2.** Statistics such as Root mean square error and Mean average percentage error for above GEM concentration for nested simulations using different emission inventories

Emission Inventory	RMSE (ng/m <sup>3</sup> )	MAPE(%)
UNEP2010	0.971	22.0
WHET	0.708	19.9
EDGAR	1.075	23.6
STREETS	0.703	19.4
UNEP2015	0.835	19.0

### 3. HG CONCENTRATIONS

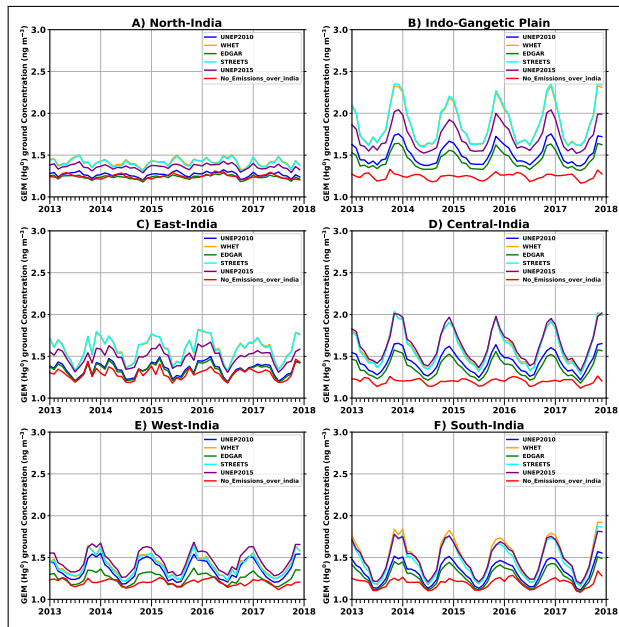


**Fig. S2.** Monthly mean variation of ground GEM ( $\text{Hg}^0$ ) concentration ( $\text{ng}/\text{m}^3$ ) during 2013-2017 for (a) North India, (b) Indo Gangetic Plain , (c) East India (d) Central India, (e) Western India, , and (f) South India respectively

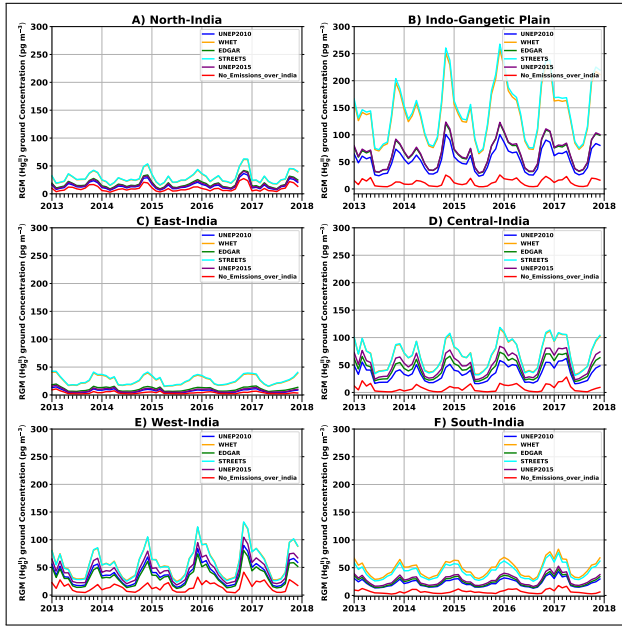


**Fig. S3.** Monthly mean variation of ground RGM ( $Hg_g^{II}$ ) concentration ( $\text{pg}/\text{m}^3$ ) during 2013-2017 for (a) North India, (b) Indo Gangetic Plain, (c) East India (d) Central India, (e) Western India, and (f) South India respectively.

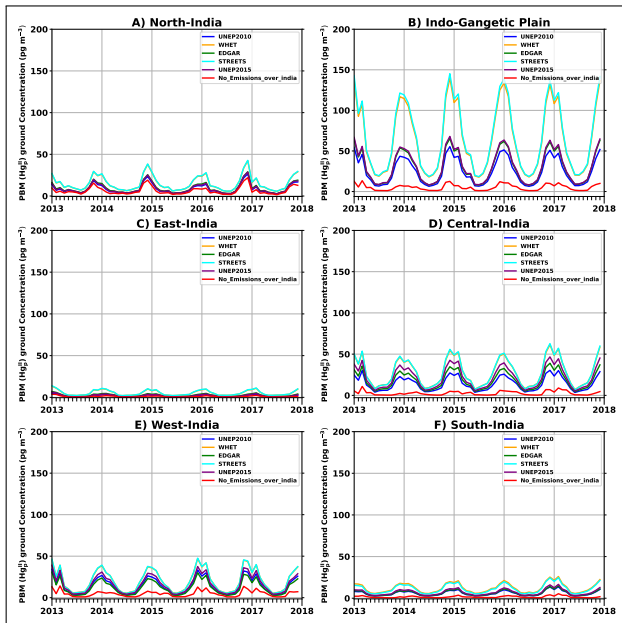


**Fig. S4.** Monthly mean variation of ground PBM ( $Hg_p^{II}$ ) concentration ( $\text{pg}/\text{m}^3$ ) during 2013-2017 for (a) North India, (b) Indo Gangetic Plain, (c) East India (d) Central India, (e) Western India, and (f) South India respectively

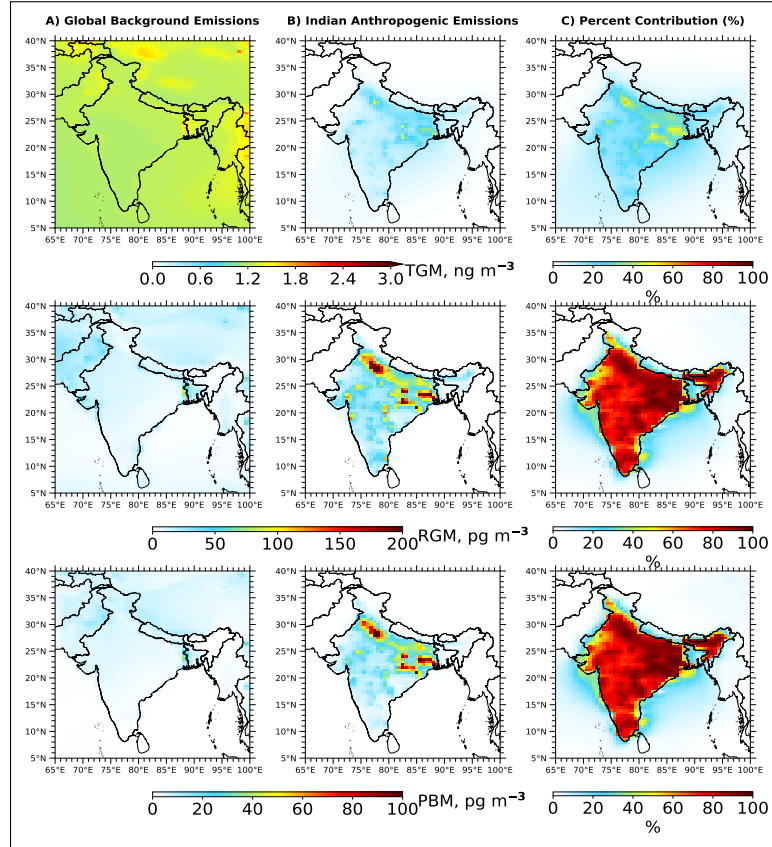


**Fig. S5.** Contributions of Indian anthropogenic emissions to Hg concentrations during 2013–2017. A) Hg concentration due to Global background and B) Absolute difference (middle row) and C) percent contribution by Indian American anthropogenic sources (right). Top row: Total Gaseous Mercury ( $\text{ng}/\text{m}^3$ ), middle row: Reactive Gaseous Mercury ( $\text{pg}/\text{m}^3$ ) and bottom row: Paticulate bound Mercury ( $\text{pg}/\text{m}^3$ )

#### 4. HG WET DEPOSITION

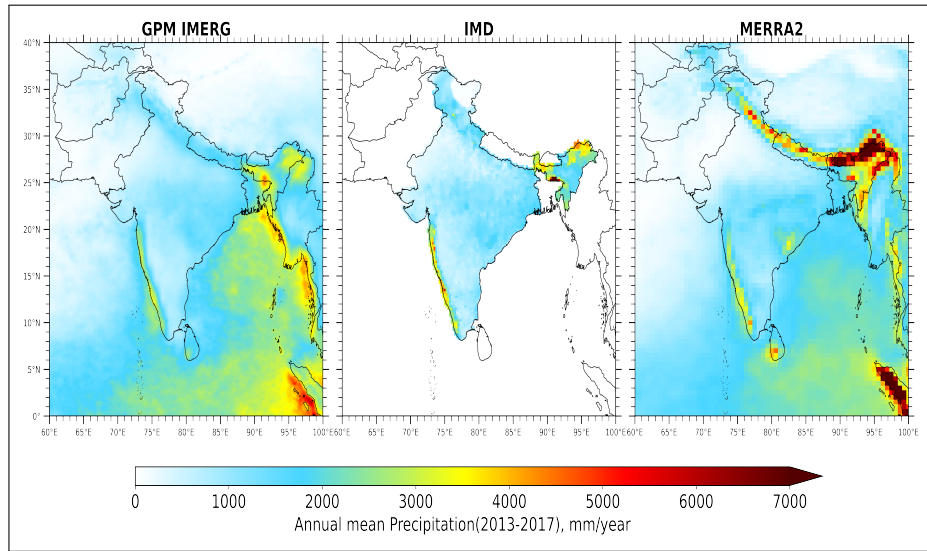


**Fig. S6.** Comparison of total annual surface precipitation between the GPI IMERG satellite datasets ( $0.1 \times 0.1$ , left column), IMD gridded rainfall dataset(Indian Meteorological Department) ( $0.25 \times 0.25^\circ$ , middle column) and MERRA2 (GEOS-Chem) ( $0.5 \times 0.625$ , right column) data during 2013-2017.

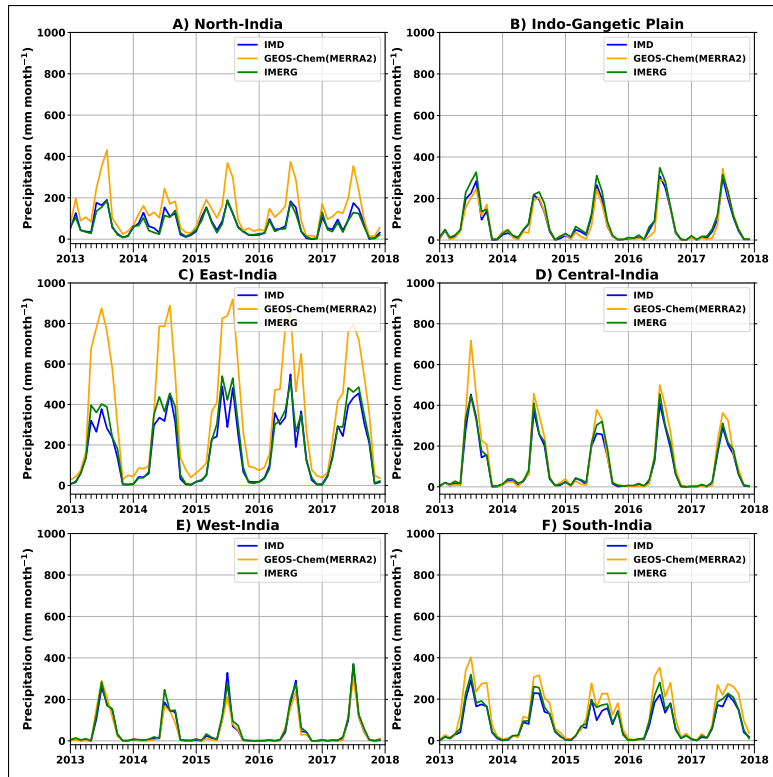


**Fig. S7.** Monthly mean variation of surface precipitation ( $\text{mm/month}$ ) during 2013-2017 for GPI IMERG satellite datasets (green line), IMD gridded rainfall dataset (Indian Meteorological Department) (blue line) and MERRA2 (GEOS-Chem) (yellow line) data for (a) North India, (b) Indo Gangetic Plain , (c) East India (d) Central India, (e) Western India , and (f) South India respectively

## 5. HG DRY DEPOSITION

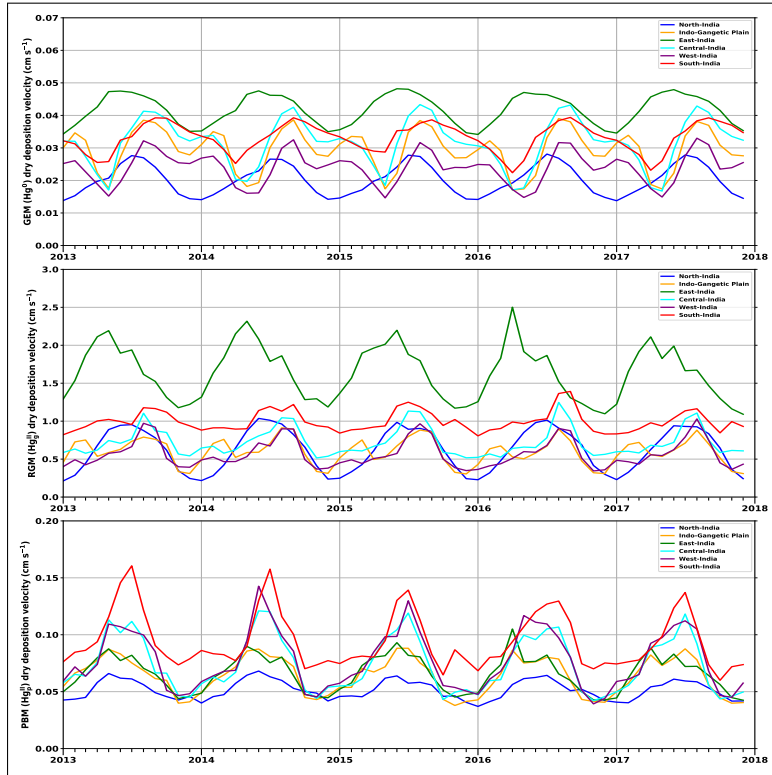


**Fig. S8.** Monthly mean variation of dry depositional velocity ( $\text{cm/s}$  during 2013-2017 for GEM ( $\text{Hg}^0$ ), RGM ( $\text{Hg}_g^{II}$ ) and PBM ( $\text{Hg}_p^{II}$ ) for (a) North India (blue color), (b) Indo Gangetic Plain (yellow color), (c) East India (green color) (d) Central India (cyan color), (e) Western India (purple color), and (f) South India (red color) respectively

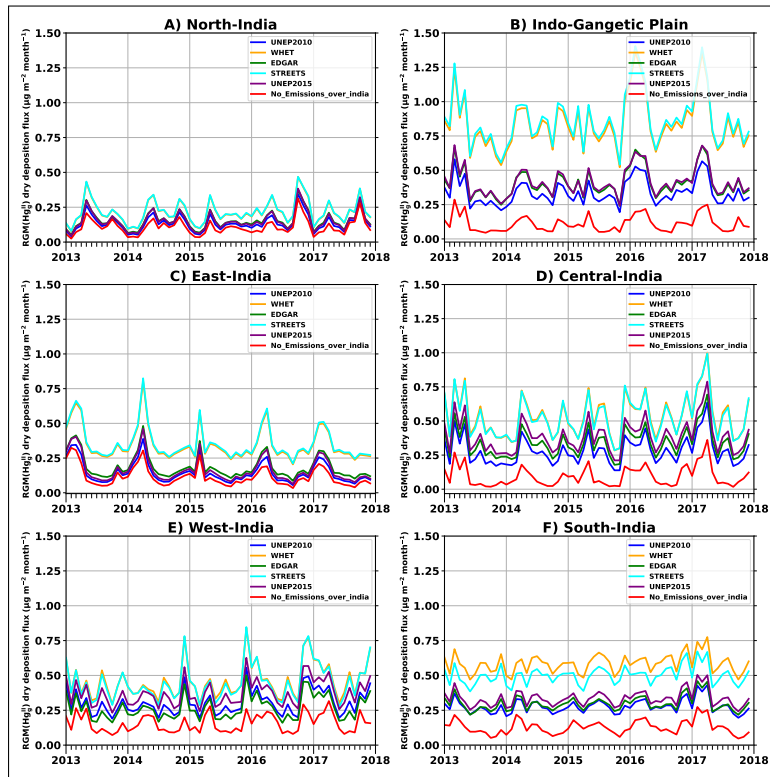


**Fig. S9.** Monthly mean variation of RGM ( $\text{Hg}_g^{\text{II}}$ ) dry deposition flux ( $\mu\text{g}/\text{m}^2/\text{month}$ ) during 2013-2017 for (a) North India, (b) Indo Gangetic Plain, (c) East India (d) Central India, (e) Western India, and (f) South India respectively.

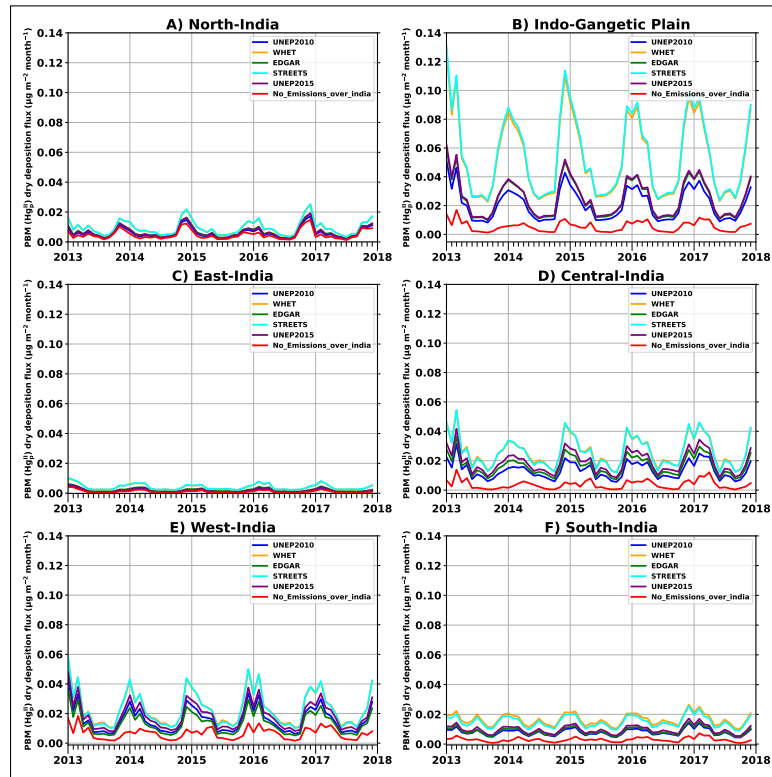


**Fig. S10.** Monthly mean variation of PBM ( $\text{Hg}^{II}$ ) dry deposition flux ( $\mu\text{g/m}^2/\text{month}$ ) during 2013-2017 for (a) North India, (b) Indo Gangetic Plain, (c) East India (d) Central India, (e) Western India, and (f) South India respectively.

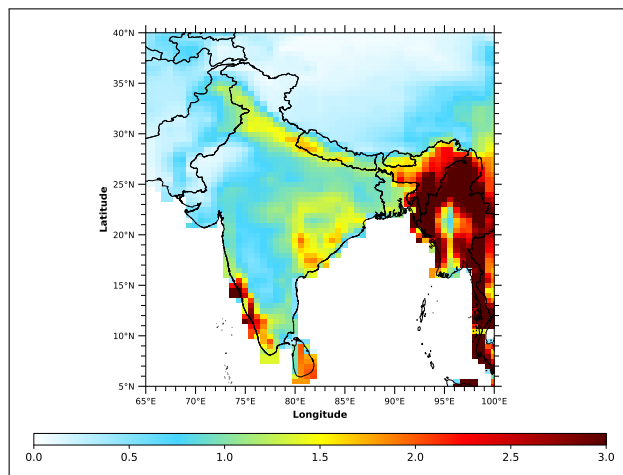


**Fig. S11.** Spatial distribution of annual average leaf area index ( $\text{m}^2/\text{m}^2$ ) during 2013-2017

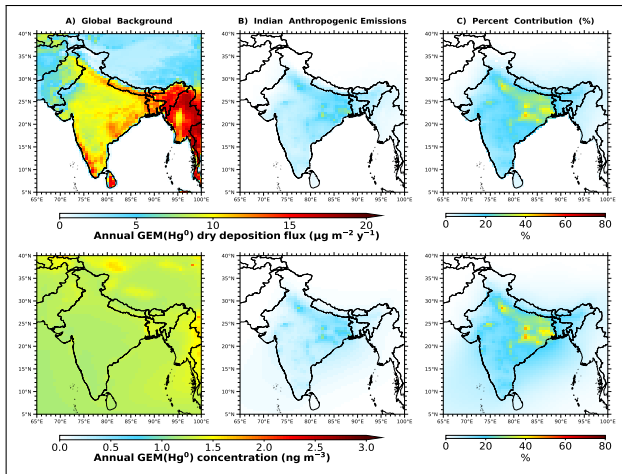


**Fig. S12.** Contributions of Indian anthropogenic emissions to GEM ( $\text{Hg}^0$ ) dry deposition and concentrations during 2013–2017. A) GEM deposition and concentration due to Global background(left) and B) Absolute difference and C) percent contribution by Indian American anthropogenic sources . Top row: GEM ( $\text{Hg}^0$ ) dry deposition ( $\text{ng}/\text{m}^3$ ), middle row:Gaseous Elemental Mercury ( $\text{pg}/\text{m}^3$ ) concentration

## REFERENCES

1. F. Sprovieri, N. Pirrone, M. Bencardino, *et al.*, “Atmospheric mercury concentrations observed at ground-based monitoring sites globally distributed in the framework of the gmos network,” *Atmospheric Chem. Phys.* **16**, 11915–11935 (2016).
2. X. W. Fu, H. Zhang, B. Yu, *et al.*, “Observations of atmospheric mercury in china: a critical review,” *Atmospheric Chem. Phys.* **15**, 9455–9476 (2015).
3. X. Fu, W. Zhu, H. Zhang, *et al.*, “Depletion of atmospheric gaseous elemental mercury by plant uptake at mt. changbai, northeast china,” *Atmospheric Chem. Phys.* **16**, 12861–12873 (2016).
4. H. Lin, Y. Tong, X. Yin, *et al.*, “First measurement of atmospheric mercury species in qomolangma natural nature preserve, tibetan plateau, and evidence of transboundary pollutant invasion,” *Atmospheric Chem. Phys.* **19**, 1373–1391 (2019).
5. B. Yu, X. Wang, C. Lin, *et al.*, “Characteristics and potential sources of atmospheric mercury at a subtropical near-coastal site in east china,” *J. Geophys. Res. Atmospheres* **120**, 8563–8574 (2015).
6. B. de Foy, Y. Tong, X. Yin, *et al.*, “First field-based atmospheric observation of the reduction of reactive mercury driven by sunlight,” *Atmospheric Environ.* **134**, 27–39 (2016).
7. C. Wang, Z. Wang, and X. Zhang, “Characteristics of the air–sea exchange of gaseous mercury and deposition flux of atmospheric mercury at an island near the boundary of the bohai sea and yellow sea,” *Atmospheric Environ.* **232**, 117547 (2020).
8. C. Wang, Z. Wang, and X. Zhang, “Two years measurement of speciated atmospheric mercury in a typical area of the north coast of china: Sources, temporal variations, and influence of regional and long-range transport,” *Atmospheric Environ.* **228**, 117235 (2020).
9. K. Liu, Q. Wu, S. Wang, *et al.*, “Improved atmospheric mercury simulation using updated gas-particle partition and organic aerosol concentrations,” *J. Environ. Sci.* **119**, 106–118 (2022).
10. L. S. P. Nguyen, G.-R. Sheu, D.-W. Lin, and N.-H. Lin, “Temporal changes in atmospheric mercury concentrations at a background mountain site downwind of the east asia continent in 2006–2016,” *Sci. The Total. Environ.* **686**, 1049–1056 (2019).
11. L. S. Phu Nguyen, L. Zhang, D.-W. Lin, *et al.*, “Eight-year dry deposition of atmospheric mercury to a tropical high mountain background site downwind of the east asian continent,” *Environ. Pollut.* **255**, 113128 (2019).
12. Y. Tang, S. Wang, Q. Wu, *et al.*, “Recent decrease trend of atmospheric mercury concentrations in east china: the influence of anthropogenic emissions,” *Atmospheric Chem. Phys.* **18**, 8279–8291 (2018).
13. Y. Zhang, R. Liu, X. Cui, *et al.*, “The characteristic analysis of atmospheric mercury during

- haze days in qingdao." *China Environ. Sci.* **34**, 1905–1911 (2014).
- 14. X. Chen, R. Balasubramanian, Q. Zhu, *et al.*, "Characteristics of atmospheric particulate mercury in size-fractionated particles during haze days in shanghai," *Atmospheric Environ.* **131**, 400–408 (2016).
  - 15. L. Duan, X. Wang, D. Wang, *et al.*, "Atmospheric mercury speciation in shanghai, china," *Sci. The Total. Environ.* **578**, 460–468 (2017).
  - 16. X. Qin, X. Wang, Y. Shi, *et al.*, "Characteristics of atmospheric mercury in a suburban area of east china: sources, formation mechanisms, and regional transport," *Atmospheric Chem. Phys.* **19**, 5923–5940 (2019).
  - 17. X. Nie, Y. Wang, H. Mao, *et al.*, "Atmospheric mercury in an eastern chinese metropolis (jinan)," *Ecotoxicol. Environ. Saf.* **196**, 110541 (2020).
  - 18. H. Yi, L. Tong, J.-m. Lin, *et al.*, "Temporal variation and long-range transport of gaseous elemental mercury (gem) over a coastal site of east china," *Atmospheric Res.* **233**, 104699 (2020).
  - 19. Y. Hong, J. Chen, J. Deng, *et al.*, "Pattern of atmospheric mercury speciation during episodes of elevated pm<sub>2.5</sub> levels in a coastal city in the yangtze river delta, china," *Environ. Pollut.* **218**, 259–268 (2016).
  - 20. Q. Hong, Z. Xie, C. Liu, *et al.*, "Speciated atmospheric mercury on haze and non-haze days in an inland city in china," *Atmospheric Chem. Phys.* **16**, 13807–13821 (2016).
  - 21. J. Zhou, Z. Wang, T. Sun, *et al.*, "Mercury in terrestrial forested systems with highly elevated mercury deposition in southwestern china: The risk to insects and potential release from wildfires," *Environ. Pollut.* **212**, 188–196 (2016).
  - 22. Q. Wu, Y. Tang, S. Wang, *et al.*, "Developing a statistical model to explain the observed decline of atmospheric mercury," *Atmospheric Environ.* **243**, 117868 (2020).
  - 23. Glob. NEST J. (2022).